Electronic Supplementary Material (ESI) for Journal of Materials Chemistry C

Bis(Carbazolyl) Derivatives of Pyrene and Tetrahydropyrene: Synthesis, Structures, Optical Properties, Electrochemistry, and Electroluminescence

Bilal R. Kaafarani,[1,*] Ala'a O. El-Ballouli,[1] Roman Trattnig,[2] Alexandr Fonari,[3] Stefan Sax,[2] Brigitte Wex,[4] Chad Risko,[5] Rony S. Khnayzer,[1] Stephen Barlow,[5] Digambara Patra,[1] Tatiana V. Timofeeva,[3] Emil J. W. List,[2,6] Jean-Luc Brédas[5] and Seth R. Marder[5]

[1]*Department of Chemistry, American University of Beirut, Beirut 1107-2020, Lebanon*
[2]*NanoTecCenter Weiz Forschungsgesellschaft mbH, Franz-Pichler-Straße 32, A-8160 Weiz, Austria*
[3]*Department of Biology &Chemistry, New Mexico Highlands University, Las-Vegas, NM 87701, USA*
[4]*Department of Natural Sciences, Lebanese American University, Byblos, Lebanon*
[5]*School of Chemistry and Biochemistry and Center for Organic Photonics and Electronics, Georgia Institute of Technology, Atlanta, Georgia 30332*
[6]*Institut für Festkörperphysik, Technische Universität Graz, Petersgasse 16, A-8010 Graz, Austria*

Table of Contents:

[*] To whom correspondence should be addressed. Email: bilal.kaafarani@aub.edu.lb; Phone: 961-3151451

Additional Crystallographic Interaction

Table S1. Crystallographic data for compounds **1a**, **2b**, **3a**, and **4b**.

Compound	**1a**	**2b**	**3a**	**4b**
Empirical formula	$C_{30}H_{20}N_2$	$C_{52}H_{56}N_2$	$C_{40}H_{28}N_2$	$C_{56}H_{56}N_2$
Formula weight	408.48	708.99	536.64	757.03
Crystal system	Orthorhombic	Monoclinic	Monoclinic	Monoclinic
Space group	*Pbca*	$P2_1/c$	$P2_1/c$	$P2_1/c$
a / Å	8.194(2)	16.051(10)	13.167(5)	17.743(2)
b / Å	16.337(5)	11.186(7)	13.192(5)	10.9925(13)
c / Å	31.464(8)	11.531(7)	8.213(3)	11.3555(14)
α / °	90	90	90	90
β / °	90	94.031(9)	106.701(7)	100.023(2)
γ / °	90	90	90	90
V / Å^3	4211.9(19)	2065(2)	1366.4(8)	2181.0(5)
Z	8	2	2	2
ρ_{calc}, g cm^{-3}	1.288	1.140	1.304	1.153
GOF on F^2	1.004	1.023	1.006	1.009
R_1; wR_2 ($I > 2\sigma(I)$)	0.0558; 0.1121	0.0501; 0.1376	0.0448; 0.0963	0.0643; 0.1320
R_1; wR_2 (all data)	0.1234; 0.1431	0.0661; 0.1578	0.0862; 0.1147	0.1318; 0.1566

Table S2. Some key angles (°) defining the conformations of **1a**, **2a**, **2b**, **3a**, and **4b** in their crystal structures.

Compound	Cent–N–aryl[a]	cbz–aryl[b]
1a[c]	176.0, 166.0	84.84(6), 57.02(8)
2a[d]	174.5	49.7
2b	168.6	74.79(36) [87.74(31)][e]
3a	175.4	53.54(5)
4b	175.2	71.48(4)

[a]Angle formed by the centroid of the five-membered ring of the carbazole, the carbazole nitrogen atom, and the ipso-carbon atom of the bridge, thus serving as a gauge of the pyramidalization of the carbazole nitrogen. [b]Angle between the best plane describing the carbazole group and that describing the adjacent bridging six-membered ring.[1] [c]The two carbazole groups are in equivalent by symmetry. [d]From ref. 2. [e]Value for major conformer present with value for minor conformer in brackets.

Molecular Torsion Angles and Nitrogen Planarity

In all four crystal structures, the coordination geometries of the carbazole nitrogen atoms are not perfectly planar: the Cent—N—C_{bridge} angles, where *Cent* is the centroid of the five-membered ring of the carbazole, (Table S2) fall short of the 180° expected for a completely planar geometry, and the sums of bond angles around the nitrogen atom are smaller than 360°. The extent of pyramidalization, gauged by either of these measures, is largest in one of the two inequivalent carbazoles of **1a** and in **2b**, but is well within the range of values that have been observed for other *N*-aryl carbazoles (for example, cent–N–aryl angles of 165.8, 169.3, 176.2, and 177.5° have been observed in 9,9'-bis(4-(3,6-di-*tert*-butylcarbazol-9-yl)phenyl)fluorene,[3] *N*-(3,5-bis(3-phenylquinoxalin-2-yl)phenyl)carbazole,[4] *N*-phenyl-(3,6-bis(4,4,5,5-tetramethyl-1,3,2-dioxaboran-2-yl)carbazole,[5] and *N*-(4-cyanophenyl)carbazole,[6] respectively). However, the nitrogen atoms in the DFT structures are all fully planarized. These geometric differences may indicate relatively shallow potential energy surfaces with respect to these distortions so that minor crystal packing effects can lead to variations.

Crystal Packing of **1a**, **2b**, **3a** and **4b**[7]

a) b)

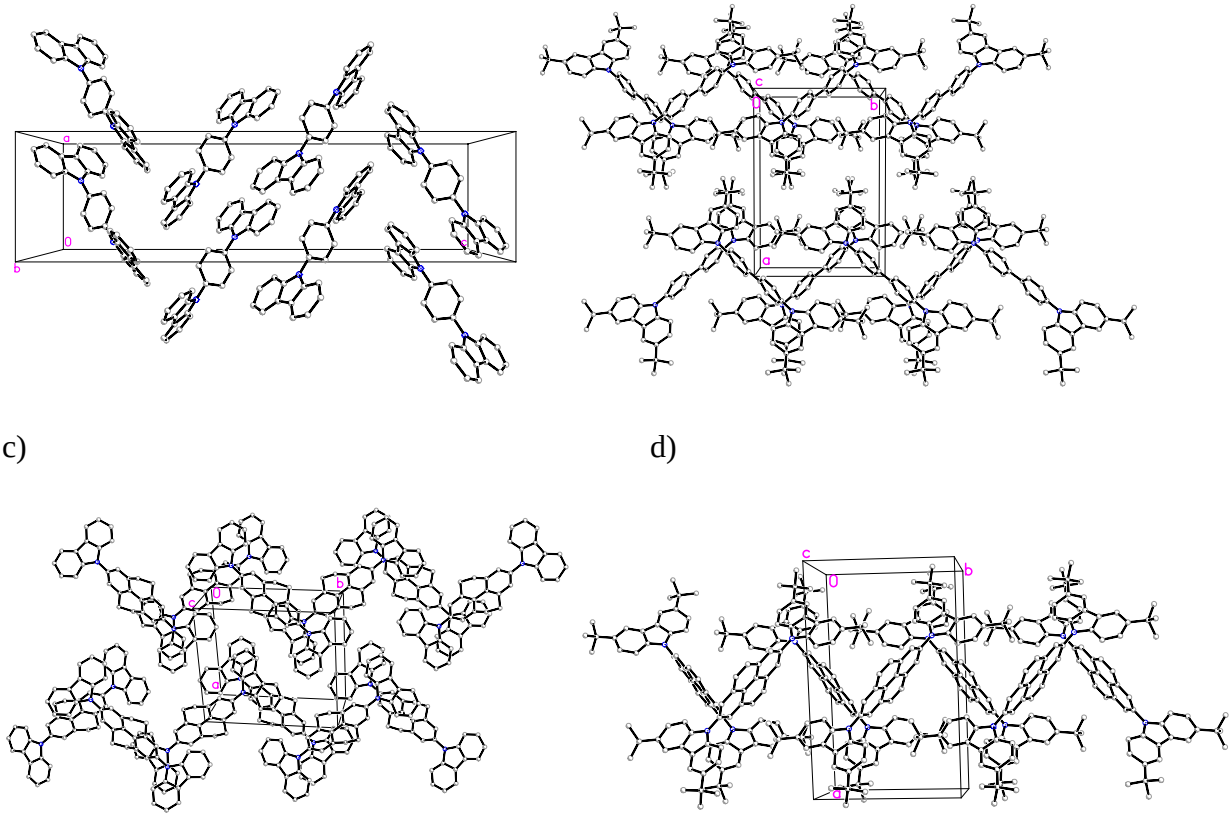

c) d)

Figure S1.Crystal packing for **1a** (a), **2b** (b), **3a** (c), and **4b**(d). Minor part of the disorder and H atoms are omitted for clarity.

Table S3. Select bond lengths (Å) and dihedral angles (°) for the ground-state neutral structures as determined at the B3LYP/6-31G(d,p) level of theory and X-ray crystallography.

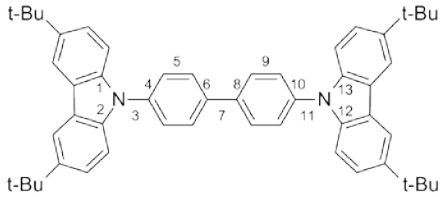

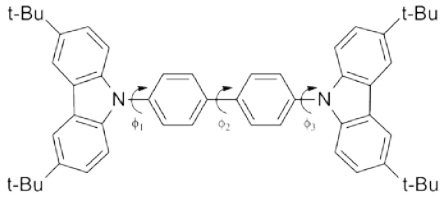

	1a	**1b**	**2b**		**3a**	**3b**	**4b**	
	expt	DFT	expt	DFT	expt	DFT	expt	DFT
bond								
1	1.396(4)	1.401	1.383(2)	1.401	1.400(3)	1.401	1.396(2)	1.401
2	1.389(4)	1.401	1.392(2)	1.401	1.392(3)	1.401	1.393(2)	1.401
3	1.428(4)	1.417	1.423(2)	1.418	1.423(2)	1.419	1.428(2)	1.419
4	1.380(4)	1.401	1.272(13)	1.401	1.382(3)	1.400	1.379(2)	1.399
5	1.391(4)	1.392	1.445(20)	1.392	1.383(3)	1.394	1.401(2)	1.402
6	1.382(4)	1.401	1.266(14)	1.405	1.395(3)	1.409	1.422(2)	1.427
7	---	---	1.484(3)	1.483	1.471(4)	1.473	1.422(3)	1.424
8	---	---	SR[#1]	1.405	SR	1.409	SR	1.427
9	---	---	SR	1.391	SR	1.394	SR	1.402
10	---	---	SR	1.401	SR	1.401	SR	1.399
11	1.422(4)	1.417	SR	1.417	SR	1.419	SR	1.419
12	1.404(4)	1.401	SR	1.401	SR	1.401	SR	1.401
13	1.402(4)	1.401	SR	1.401	SR	1.401	SR	1.401
angle								
φ_1[#2]	84.84(6)	53.4	74.79(36) [87.74(31)]	53.3	53.54(5)	53.7	71.48(4)	53.8
φ_2[#2]	---	---	0	37.0	0	16.8	0	0.0
φ_3[#2]	57.02(8)	53.4	SR	52.5	SR	53.4	SR	53.8

[#1]Symmetry related; [#2]same values for experimental columns as in Table 2 from the main text.

Table S4. Select bond lengths (Å) and dihedral angles (°) for the radical-cation states as determined at the B3LYP/6-31G(d,p) level of theory. Change in bond length (Δ, Å) on going to the radical cation state is also provided. The relaxation energy on going from the radical-cation to the neutral state (λ_1), neutral to radical-cation state (λ_2), and total intramolecular reorganization energy (λ_t) are also provided.

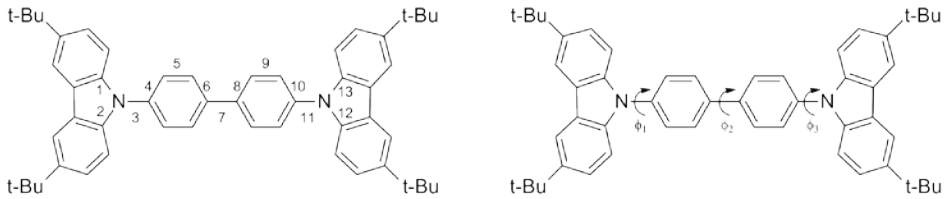

	1b		**2b**		**3b**		**4b**	
	DFT	Δ	DFT	Δ	DFT	Δ	DFT	Δ
bond								
1	1.410	0.009	1.406	0.005	1.409	0.008	1.404	0.003
2	1.410	0.009	1.405	0.004	1.409	0.008	1.404	0.003
3	1.399	-0.018	1.407	-0.011	1.403	-0.016	1.412	-0.007
4	1.410	0.009	1.406	0.005	1.408	0.008	1.403	0.004
5	1.383	-0.009	1.386	-0.006	1.386	-0.008	1.398	-0.004
6	1.410	0.009	1.410	0.005	1.418	0.009	1.431	0.004
7	---	---	1.472	-0.011	1.457	-0.016	1.418	-0.006
8	---	---	1.411	0.006	1.418	0.009	1.431	0.004
9	---	---	1.386	-0.005	1.387	-0.007	1.398	-0.004
10	---	---	1.407	0.006	1.408	0.007	1.403	0.004
11	1.399	-0.018	1.406	-0.011	1.403	-0.016	1.412	-0.007
12	1.410	0.009	1.406	0.005	1.409	0.008	1.404	0.003
13	1.410	0.009	1.406	0.005	1.409	0.008	1.404	0.003
angle								
φ_1	42.9	-10.5	46.4	-6.9	44.0	-9.7	47.9	-5.9
φ_2	---	---	29.9	-7.1	16.1	-0.7	0.0	0.0
φ_3	42.9	-10.5	45.2	-7.3	44.3	-9.1	47.9	-5.9
reorganization energy								
λ_1	0.089		0.059		0.078		0.046	
λ_2	0.087		0.053		0.072		0.044	
λ_t	0.176		0.112		0.150		0.090	

Photophysical Studies

Fluorescence quantum yield (Φ_f) represents the fraction of excited molecules that fluoresce; since energetic losses may prevent some of the excited molecules from returning to the ground state by fluorescence.[8] Fluorescence quantum yields were determined in different solvents by comparison to a standard of known quantum yield, according to the following equation:[9]

$$\Phi_{unk} = \Phi_{std}\frac{F_{unk}}{F_{std}}\frac{A_{std}}{A_{unk}}\frac{n_{unk}^2}{n_{std}^2}$$

where standard (std) refers to the reference sample (i.e. anthracene in ethanol at 2 μM concentration) and unkown (unk) refers to compounds (**1-4**). For instance, Φ_{unk} and $\Phi_{std}$are the quantum yields of the sample of interest and the reference, respectively. The quantum yield of anthracene in ethanol was taken as 0.31.[10] *F* corresponds to the integrated intensity of the emission spectra of the sample or reference, while *A* is the optical density of the sample or reference at the excitation wavelength, i.e. 330 or 320 nm. Finally, *n* is the refractive index of the solvent being used. Quantum yield calculations were done using 1 μM solutions of each compound in different solvents. The obtained results are summarized in Table S5, which presents the quantitative data for emission maximum and fluorescence quantum yield calculations.

Table S5. Absorption and emission maxima, Stokes shift and fluorescence quantum yields for **1-4** in various solvents.

Compound	Solvent	λ_{abs}^{max} (nm)	λ_{em}^{max} (nm)	Stokes shift (cm^{-1})	Φ_f
1a	ACN	341	363	1777	0.53
	Cyclohex	338	342	346	0.50
	DCM	341	363	1777	0.33
	DMF	340	363	1864	0.46
	EtOH	341	360	1548	0.38
	Hex	338	342	346	0.10
	MeOH	--	--	--	--
	THF	340	361	1710	0.28
1b	ACN	345	371	2031	0.19
	Cyclohex	345	352	576	0.22
	DCM	347	376	2223	0.10
	DMF	346	371	1948	0.24
	EtOH	345	368	1812	0.13
	Hex	345	351	495	0.17
	MeOH	--	--	--	--
	THF	346	370	1875	0.14
2a	ACN	338	394	4205	0.49
	Cyclohex	340	351	922	0.23
	DCM	341	369	2225	0.32
	DMF	340	387	3572	0.42
	EtOH	340	369	2311	0.75
	Hex	340	351	922	0.25
	MeOH	339	384	3457	0.43
	THF	340	379	3027	0.36
2b	ACN	---	408	--	--
	Cyclohex	347	364	1346	0.36
	DCM	347	397	3630	0.55
	DMF	347	404	4066	0.15
	EtOH	346	393	3456	0.12
	Hex	346	363	1354	0.39
	MeOH	346	398	3776	0.10
	THF	---	390	---	--
3a	ACN	336	379	3377	0.06
	Cyclohex	340	376	2816	0.09
	DCM	336	380	3446	0.28
	DMF	341	381	3079	0.49
	EtOH	338	377	3061	0.12
	Hex	340	375	2745	0.27
	MeOH	---	377	---	0.08

	THF	340	378	2957	0.36
3b	ACN	349	390	3012	0.70
	Cyclohex	351	365	1093	0.25
	DCM	348	384	2694	0.43
	DMF	349	389	2946	0.69
	EtOH	349	385	2679	0.58
	Hex	351	364	1018	0.82
	MeOH	350	386	2665	0.31
	THF	350	372	1690	0.43
4a	ACN	341	429	6015	0.29
	Cyclohex	341	413	5112	0.41
	DCM	343	425	5625	0.34
	DMF	343	429	5844	0.44
	EtOH	341	421	5573	0.35
	Hex	341	413	5112	0.24
	MeOH	341	423	5685	0.38
	THF	343	421	5402	0.43
4b	ACN	341	451	7153	0.14
	Cyclohex	344	423	5429	0.49
	DCM	344	445	6598	0.56
	DMF	341	450	7103	0.42
	EtOH	---	419	---	0.51
	Hex	344	422	5373	0.27
	MeOH	---	438	---	0.07
	THF	344	436	6134	0.40

Fluorescence Lifetime Studies

The inverse of fluorescence lifetime ($1/\tau_f$) represents the rate of total decay (k_{tot}). The measurement of τ_f, in addition to Φ_f, allow the estimation of a number of important parameters such as the radiative (k_r) and non-radiative (k_{nr}) rate constants.[8] For instance, the rate constant for radiative decay (k_r) can be calculated by the following equation:[11]

$$k_r = \frac{\Phi_f}{\tau_f}$$

while k_{nr}, which represents the average non-radiative rate constant resulting from radiationless processes such as internal conversion to the ground state and intersystem crossing to the triplet state, can be evaluated by[11]

$$k_{nr} = k_{tot} - k_r$$

Table S6 lists the fluorescence lifetimes, average fluorescence lifetimes, radiative and non-radiative rate constants of **1-4** in various solvents.

Table S6. Fluorescence lifetimes, average fluorescence lifetimes, radiative and non-radiative rate constants of **1-4** in various solvents. k_r and k_{nr} calculations were done using τ_1 for monoexponential decays, while τ_{avg} was used for biexponential decays.[a]

Compound	Solvent	τ_1/ ns (%)	τ_2/ ns (%)	τ_{avg}/ns	χ^2	k_r / 10^8 s^{-1}	k_{nr}/ 10^8 s^{-1}
1a	ACN	5.26	--	--	1.89	1.01	0.89
	Cyclohex	5.36	--	--	1.89	0.93	0.94
	DCM	4.43	--	--	1.55	0.74	1.51
	DMF	6.56	--	--	1.50	0.70	0.82
	EtOH	5.60	--	--	1.43	0.67	1.11
	Hex	3.73	--	--	1.41	0.26	2.42
	MeOH	12.9 (54%)	4.45 (46%)	8.67	1.43	--	--
	THF	5.32	--	--	1.20	0.53	1.35
1b	ACN	5.72	--	5.73	1.30	0.33	1.41
	Cyclohex	12.9 (62%)	3.88 (37%)	8.41	1.53	0.26	0.93
	DCM	3.65 (32%)	9.99 (68%)	6.82	1.39	0.14	1.32
	DMF	13.2 (53%)	5.73 (47%)	9.47	1.45	0.25	0.81
	EtOH	22.7 (33%)	5.57 (66%)	1.42	1.32	0.09	0.61
	Hex	12.2 (28%)	3.82 (72%)	8.02	1.68	0.21	1.04
	MeOH	12.8 (49%)	4.34 (51%)	8.57	1.31	--	--
	THF	3.17 (20%)	8.70 (80%)	5.94	1.31	0.23	1.46
2a	ACN	2.69	--	--	1.40	1.82	1.90
	Cyclohex	1.53	--	--	1.44	1.50	5.03
	DCM	1.97	--	--	1.48	1.62	3.44
	DMF	2.50	--	--	1.69	1.68	2.32
	EtOH	2.16	--	--	1.43	3.48	1.16
	Hex	1.50	--	--	1.17	1.69	5.07
	MeOH	2.43	--	--	1.54	1.76	2.34
	THF	1.92	--	--	1.38	1.88	3.33
2b	ACN	3.26	--	--	1.70	--	--
	Cyclohex	1.53	--	--	1.48	2.36	4.19
	DCM	2.39	--	--	1.85	2.30	1.89
	DMF	3.05	--	--	1.73	0.49	2.78
	EtOH	2.56	--	--	1.79	0.47	3.44
	Hex	1.43	--	--	1.78	2.72	4.25
	MeOH	3.01	--	--	1.78	0.33	2.94
	THF	2.06	--	--	1.53	--	--
3a	ACN	2.06	--	--	1.82	0.30	4.55
	Cyclohex	1.40	--	--	1.98	0.64	6.51
	DCM	1.87	--	--	1.96	1.48	3.87
	DMF	1.95	--	--	1.98	2.52	2.62

	EtOH	1.75	--	--	1.81	0.68	5.05
	Hex	1.32	--	--	1.99	2.04	5.51
	MeOH	1.92	--	--	1.89	0.43	4.79
	THF	1.71	--	--	1.93	2.07	3.76
3b	ACN	2.15 (79%)	10.1 (20%)	6.13	1.15	1.15	0.48
	Cyclohex	1.49 (66%)	8.88 (34%)	5.19	1.60	0.48	1.44
	DCM	1.89 (47%)	9.05 (52%)	5.47	1.38	0.79	1.03
	DMF	2.03 (56%)	0.12 (44%)	6.81	1.49	1.01	0.46
	EtOH	2.01 (47%)	9.56 (53%)	5.78	1.62	0.99	0.73
	Hex	1.38 (70%)	5.63 (30%)	3.51	1.58	2.33	0.52
	MeOH	2.69 (25%)	9.65 (74%)	6.17	1.40	0.50	1.12
	THF	1.87 (42%)	9.26 (58%)	5.57	1.38	0.78	1.02
4a	ACN	2.73 (~1%)	14.9 (99%)	8.85	2.57	0.33	0.80
	Cyclohex	2.13 (~1%)	18.8 (99%)	10.5	2.89	0.39	0.56
	DCM	1.93 (~1%)	23.8 (99%)	12.8	3.08	0.27	0.51
	DMF	2.78 (~1%)	24.7 (99%)	13.8	2.45	0.32	0.40
	EtOH	2.40 (~1%)	19.2 (99%)	10.8	2.67	0.33	0.60
	Hex	2.04 (~1%)	11.8 (99%)	6.95	2.10	0.34	1.10
	MeOH	1.99 (~1%)	16.8 (99%)	9.43	2.49	0.41	0.66
	THF	2.67 (~1%)	18.9 (99%)	10.8	2.83	0.40	0.53
4b	ACN	11.9	--	--	1.66	0.12	0.72
	Cyclohex	18.4	--	--	2.38	0.26	0.28
	DCM	22.6	--	--	2.46	0.25	0.19
	DMF	18.9	--	--	1.87	0.23	0.30
	EtOH	17.2	--	--	1.95	0.29	0.29
	Hex	11.2	--	--	1.72	0.24	0.65
	MeOH	14.2	--	--	1.86	0.05	0.65
	THF	17.9	--	--	2.09	0.23	0.33

[a]No quantum yields were calculated for compounds with low solubility in particular solvents, thus k_{nr} and k_r in these solvents were not calculated.

Electronic structure and low-lying excited-state transitions

Illustrations of the frontier molecular orbitals involved in the low-lying excited-states of **1b** – **3b** and **4b** are depicted in Figures S2 and S3, respectively.

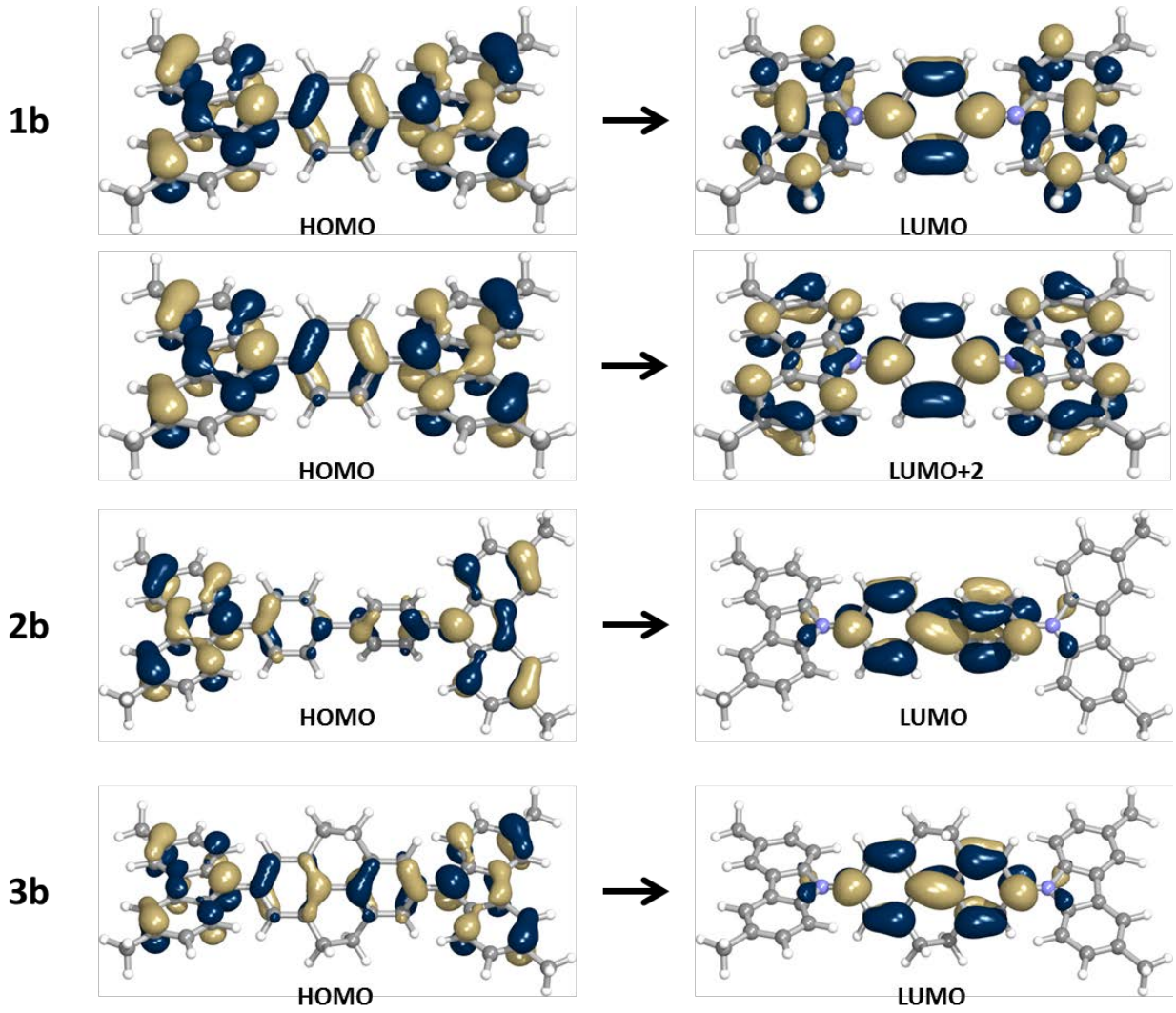

Figure S2. Illustrations of the frontier molecular orbitals involved in the $S_1 \leftarrow S_0$ vertical transitions of **1b** – **3b** as determined at the B3LYP/6-31G(d,p) level of theory.

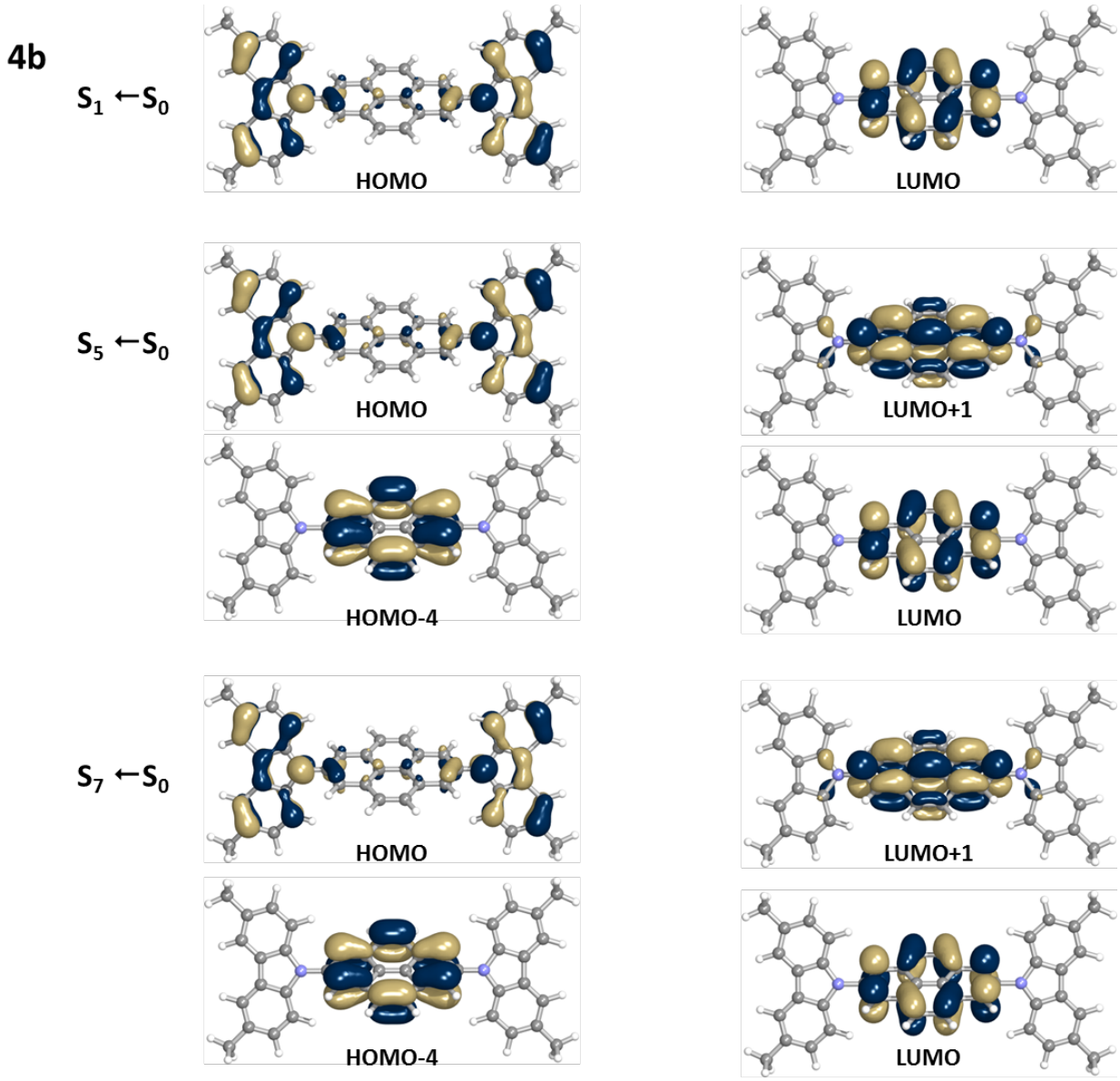

Figure S3. Illustrations of the frontier molecular orbitals involved in select low-lying vertical transitions of **4b** as determined at the B3LYP/6-31G(d,p) level of theory.

Electrochemistry

CV plots of compounds (**1-3**) are summarized in Figures S4-S6 (CV plots of **1a** and **1b** are shown in the manuscript).

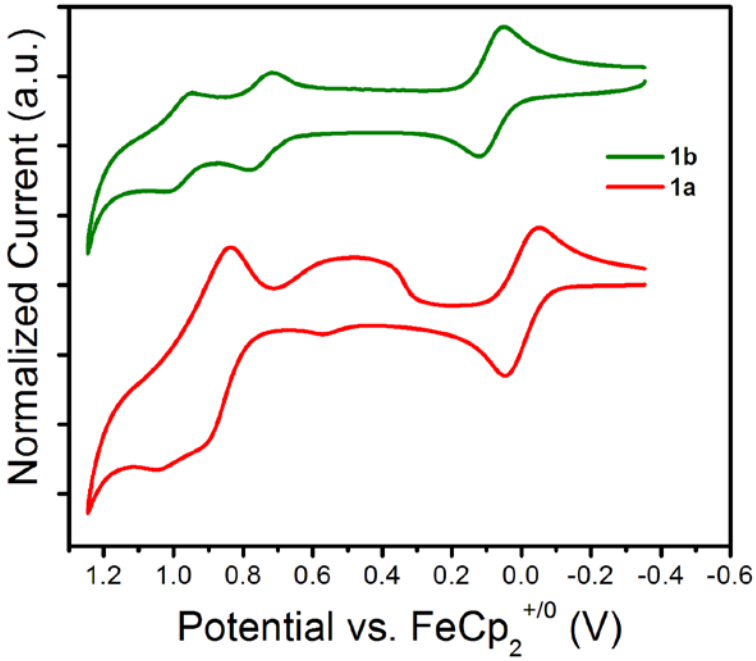

Figure S4. Cyclic Voltammograms (50 mVs^{-1}) for 1,4-bis(carbazol-9-yl)benzene (**1a**) and 1,4-bis(3,6-di-*tert*-butylcarbazol-9-yl)benzene (**1b**) with ferrocene as an internal standard in CH_2Cl_2/0.1 M $^nBu_4NPF_6$.

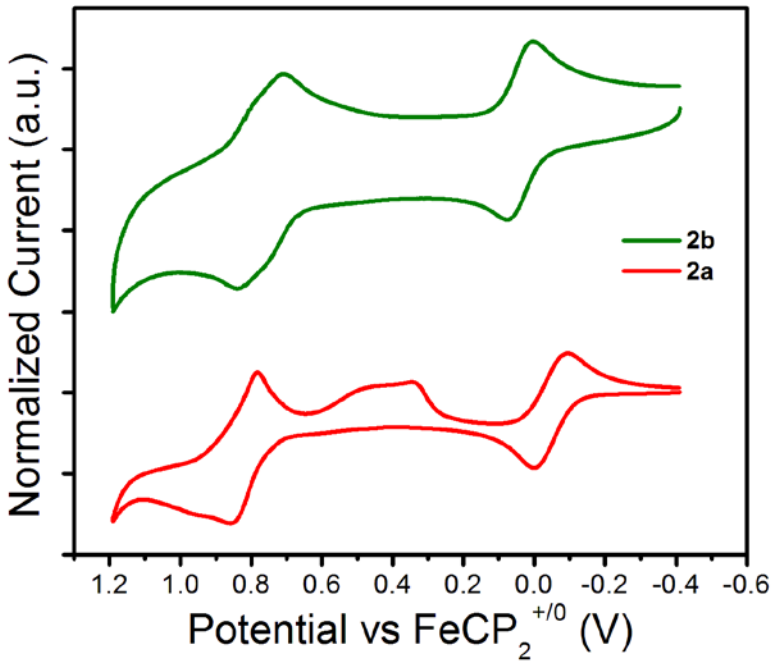

Figure S5. Cyclic Voltammograms (50 mVs^{-1}) for 1,4-bis(carbazol-9-yl)biphenyl (**2a**) and 1,4-bis(3,6-di-*tert*-butylcarbazol-9-yl)biphenyl (**2b**) with ferrocene as an internal standard in CH_2Cl_2/0.1 M $^nBu_4NPF_6$.

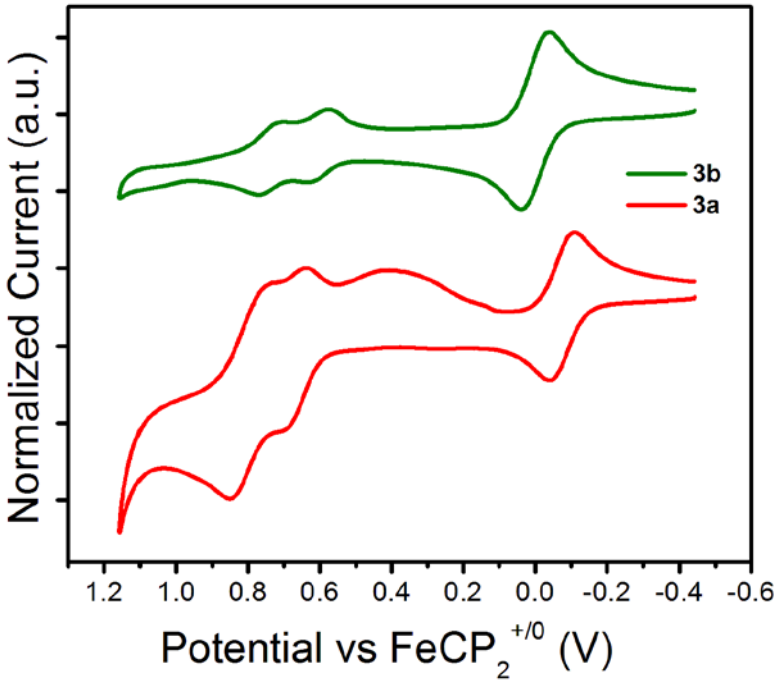

Figure S6. Cyclic Voltammograms (50 mVs^{-1}) for 1,4-bis(carbazol-9-yl)tetrahydropyrene (**3a**) and 1,4-bis(3,6-di-*tert*-butylcarbazol-9-yl)tetrahydropyrene (**3b**) with ferroceneas an internal standard in CH_2Cl_2/0.1 M $^nBu_4NPF_6$.

Differential Scanning Calorimetry Studies

Figures S7-S12 show the collected DSC curves (2nd heating and 1st cooling) for compounds **1-(a, b)**, **2(a, b)**, **3a** and **4a** upon heating to a maximum of 450 ºC and cooling to 0 ºC. However, the thermal properties of the pyrene/tetrahydropyrene-based di-*tert*-butylcarbazole derivatives (**3b** and **4b**) were not determined since no peaks were revealed even upon heating to 500 ºC. The area under the DSC curves was integrated using TA analysis in order to find $\Delta H_{melting}$ and $\Delta H_{crystallization}$.

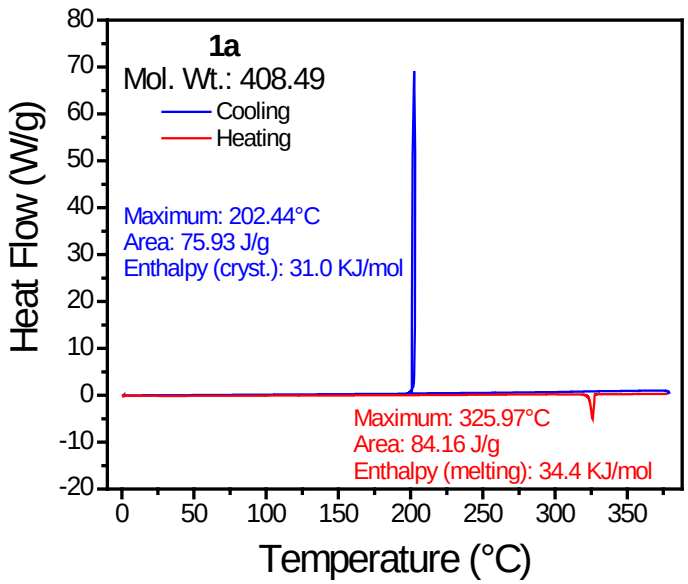

Figure S7. DSC curves of 1,4-bis(carbazol-9-yl)benzene (**1a**).

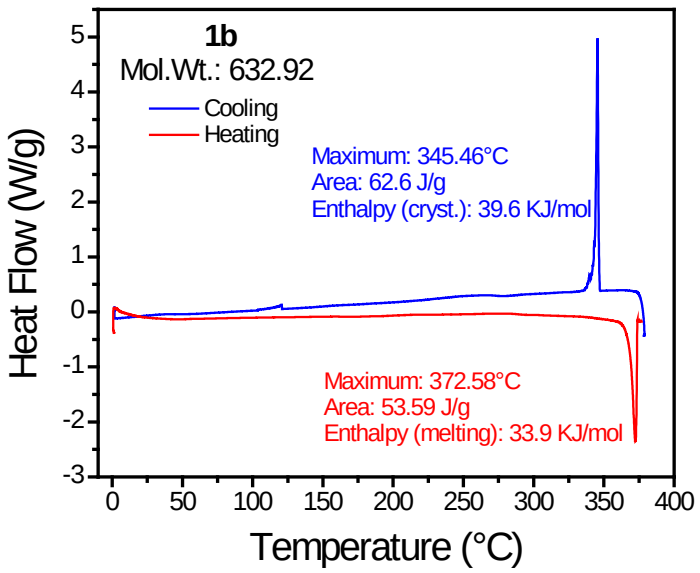

Figure S8. DSC curves of 1,4-bis(di-*tert*-butylcarbazol-9-yl)benzene (**1b**).

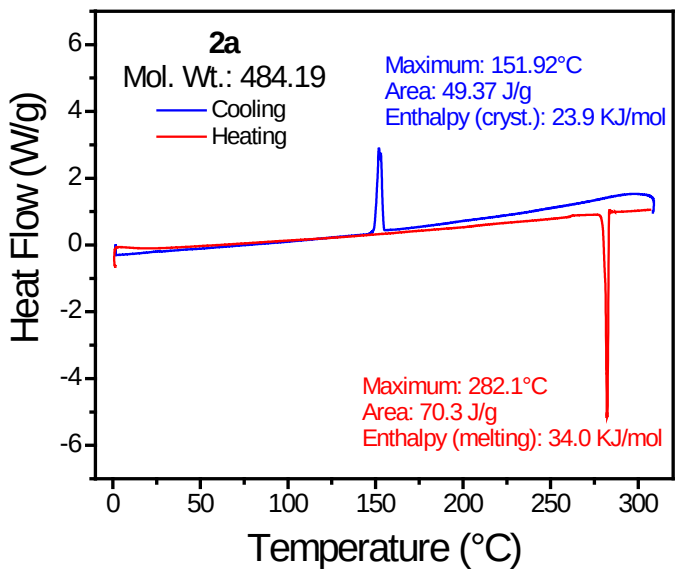

Figure S9. DSC curves of 4,4'-bis(carbazol-9-yl)biphenyl (**2a**).

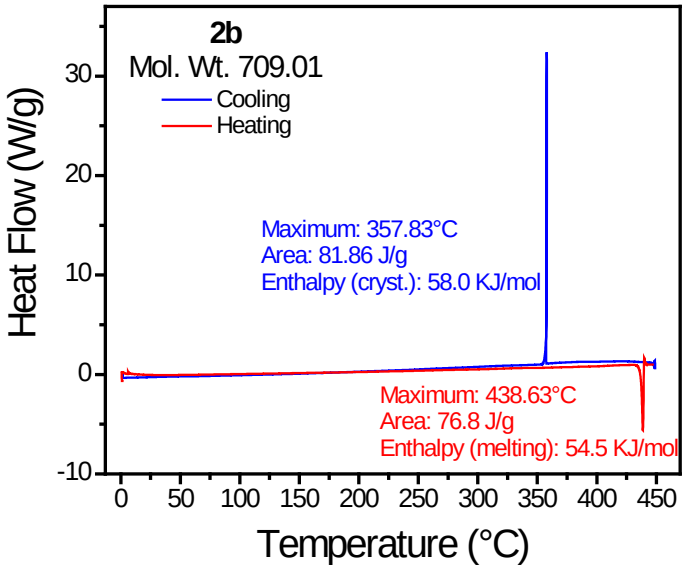

Figure S10. DSC curves of 4,4'-bis(di-*tert*-butylcarbazol-9-yl)biphenyl (**2b**).

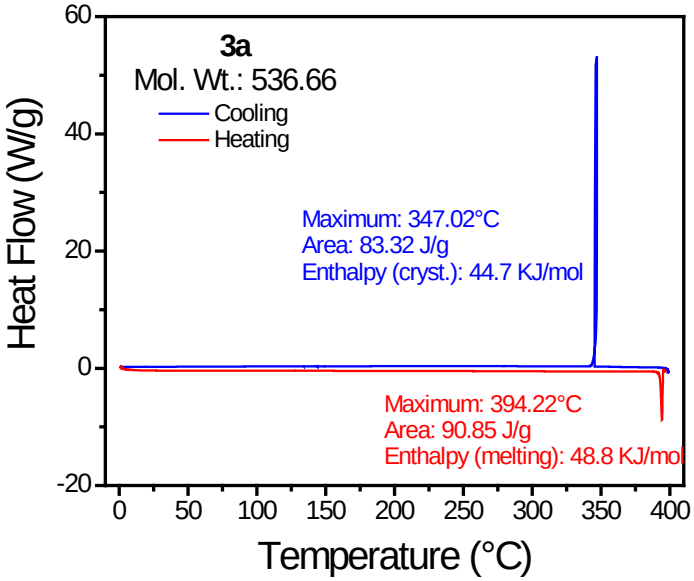

Figure S11. DSC curves of 2,7-bis(carbazol-9-yl)tetrahydropyrene (**3a**).

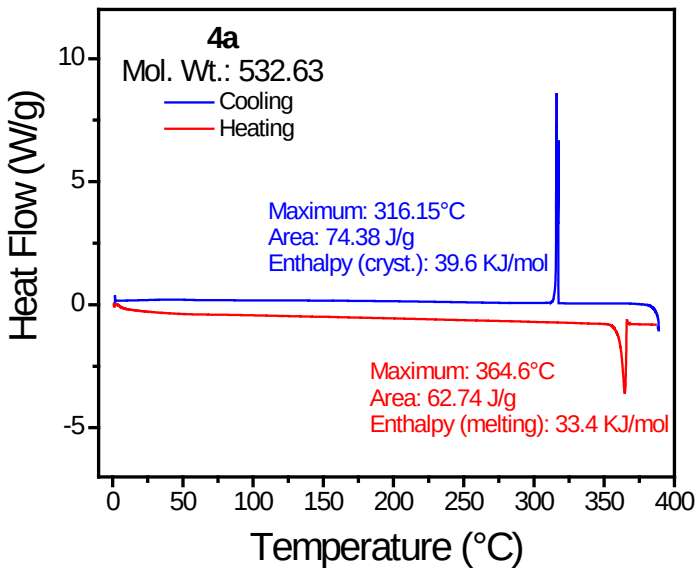

Figure S12. DSC curves of 2,7-bis(carbazol-9-yl)pyrene (**4a**).

NMR Spectroscopy

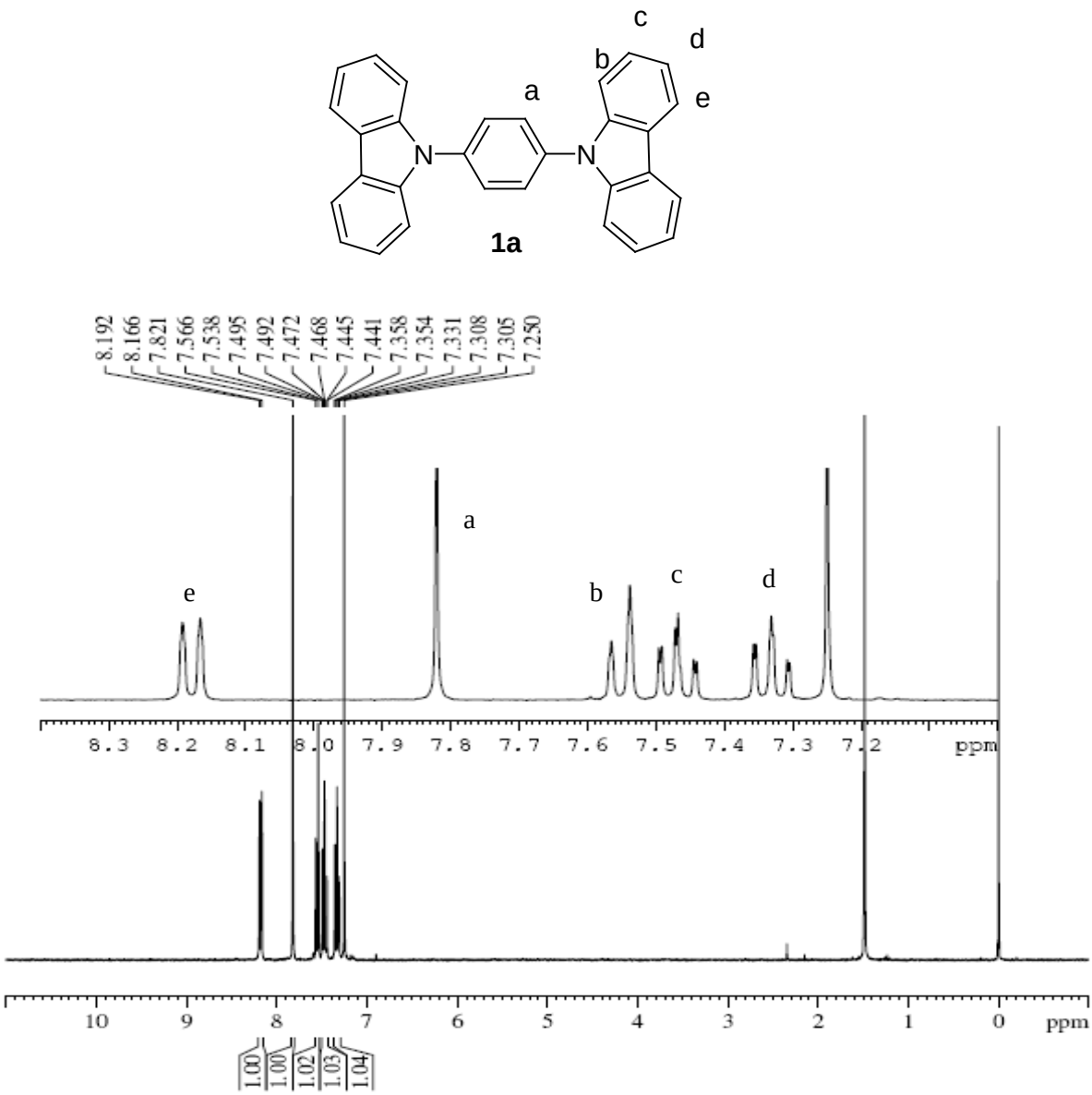

Figure S13. ^{1}H NMR of 1,4-bis(carbazol-9-yl)benzene (**1a**) in $CDCl_3$.

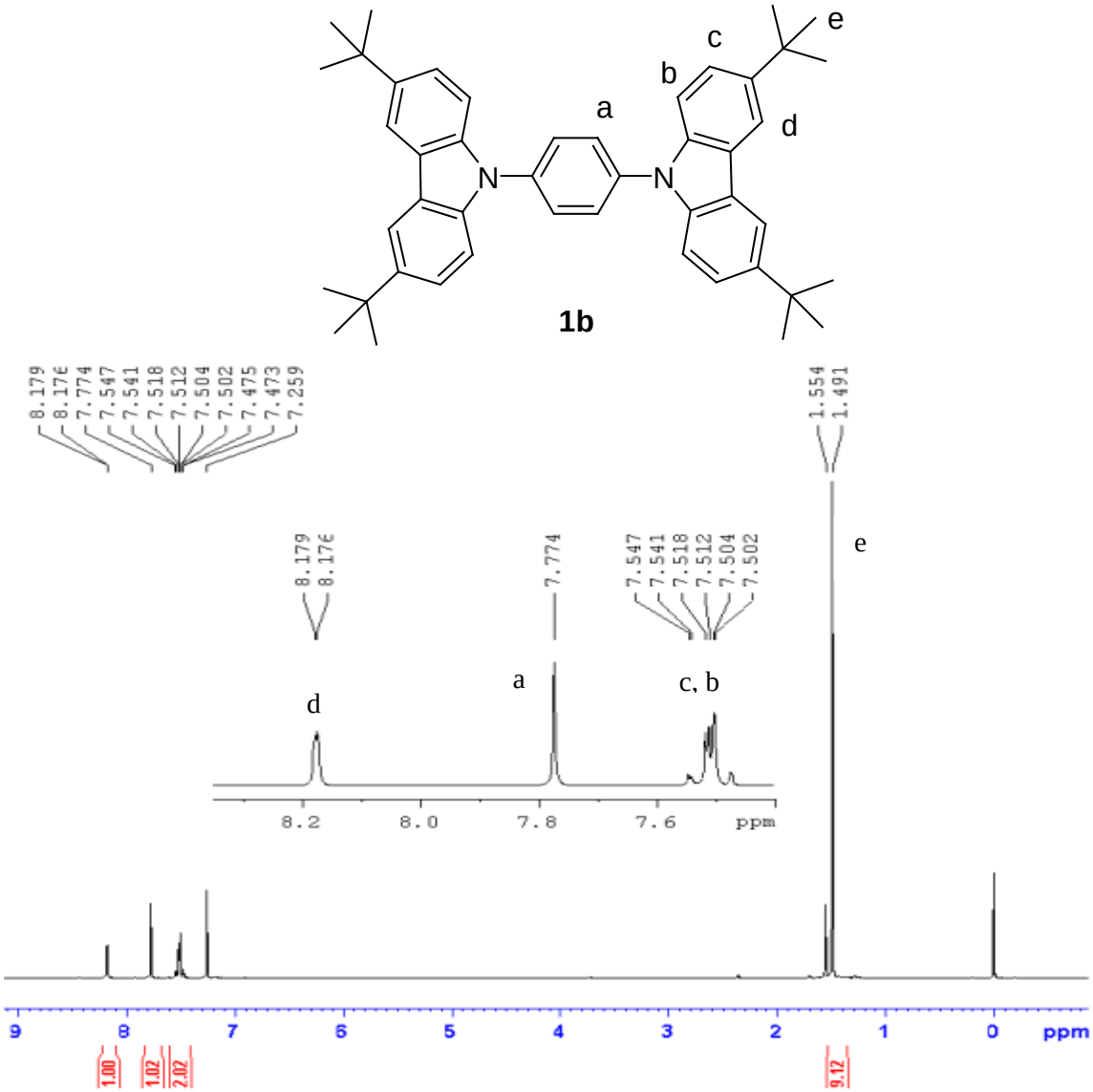

Figure S14. ^{1}H NMR of 1,4-bis(3,6-di-*tert*-butyl-9-carbazoyl)benzene (**1b**) in $CDCl_3$.

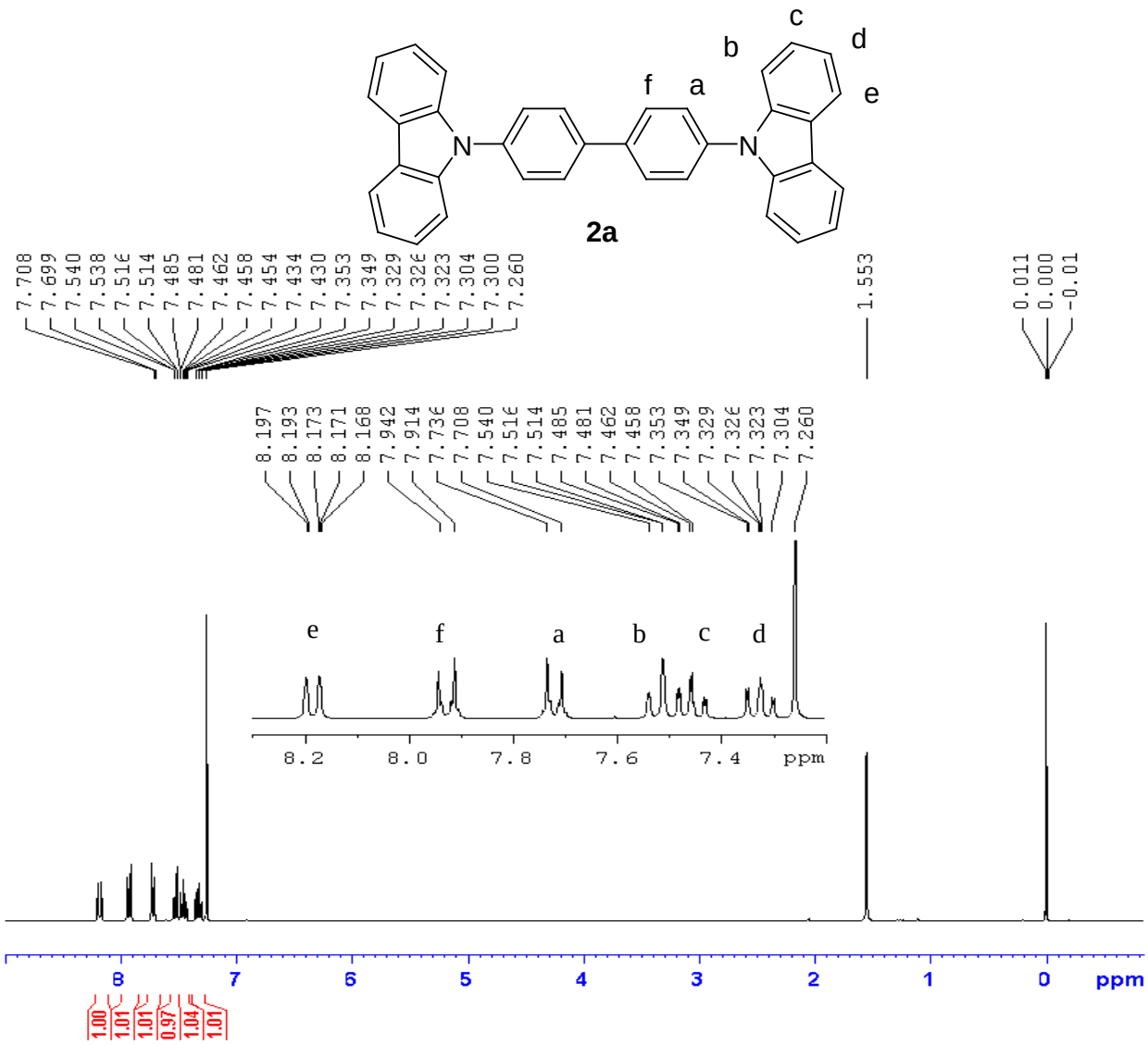

Figure S15.^{1}H NMR of 4,4'-bis(carbazol-9-yl)biphenyl(**2a**) –CBP- in $CDCl_3$.

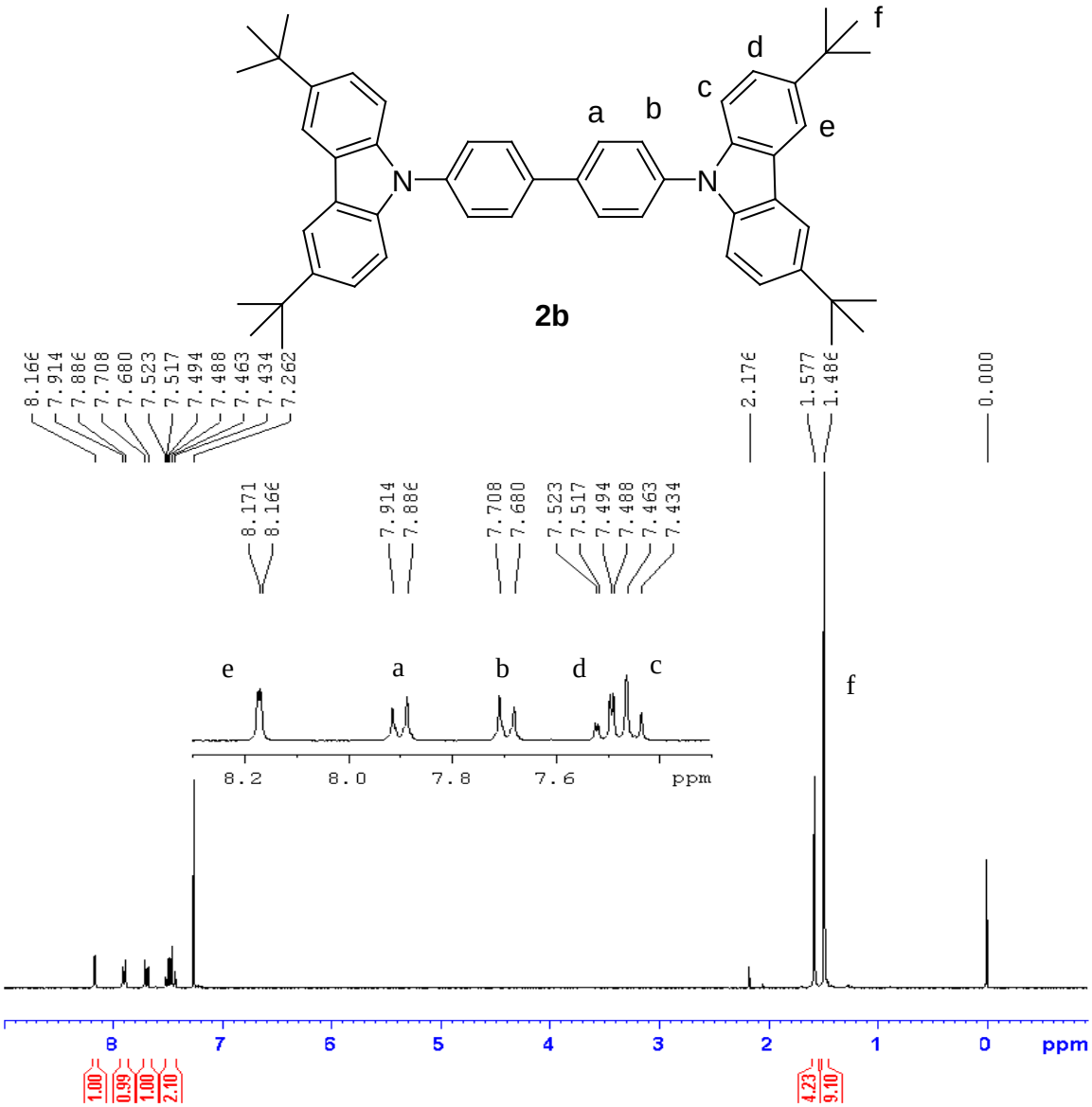

Figure S16. ^{1}H NMR of 4,4'-bis(di-*tert*-butylcarbazol-9-yl)biphenyl (**2b**) in $CDCl_3$.

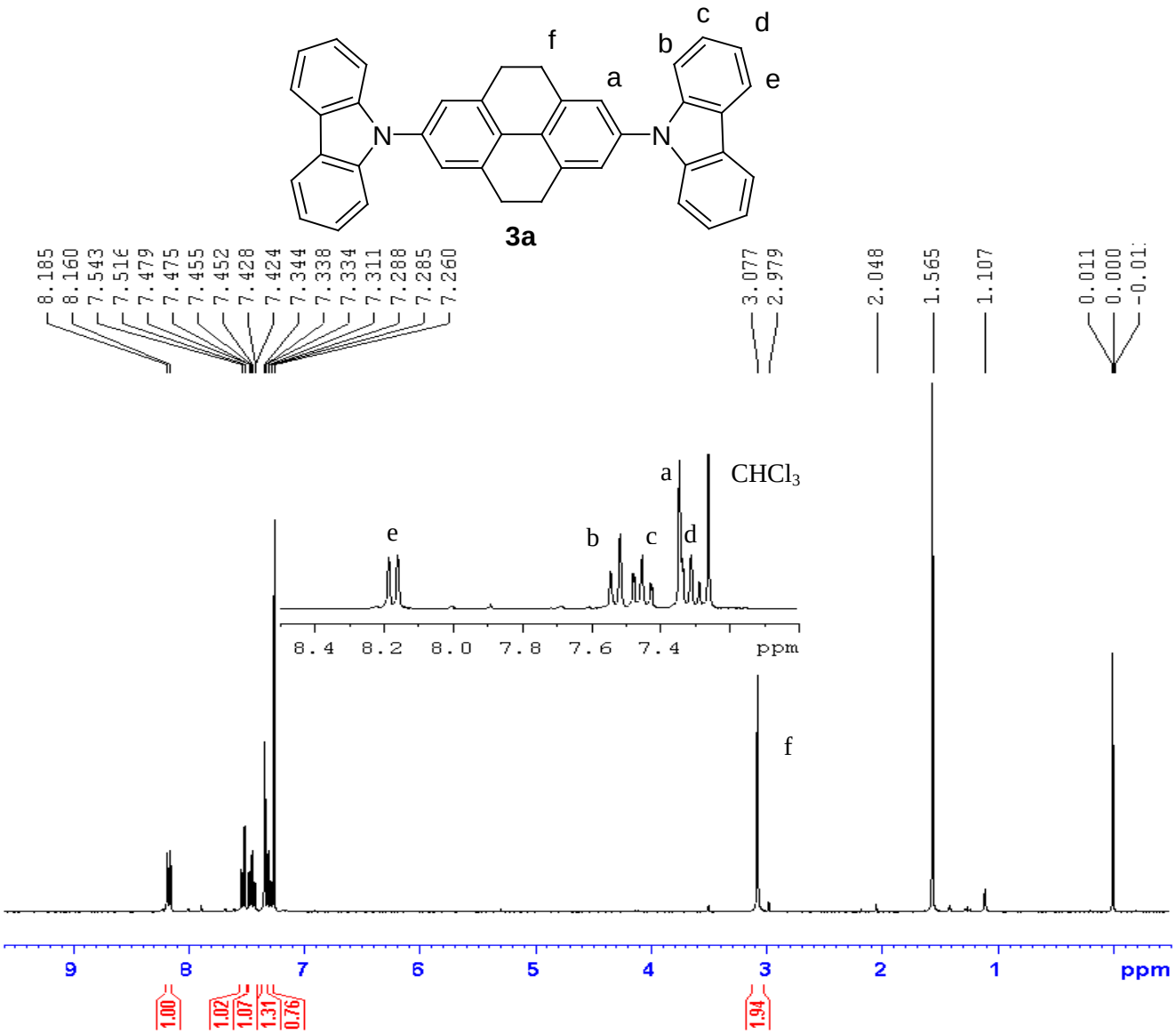

Figure S17. ^{1}H NMR of 2,7-bis(carbazol-9-yl)tetrahydropyrene (**3a**) in $CDCl_3$.

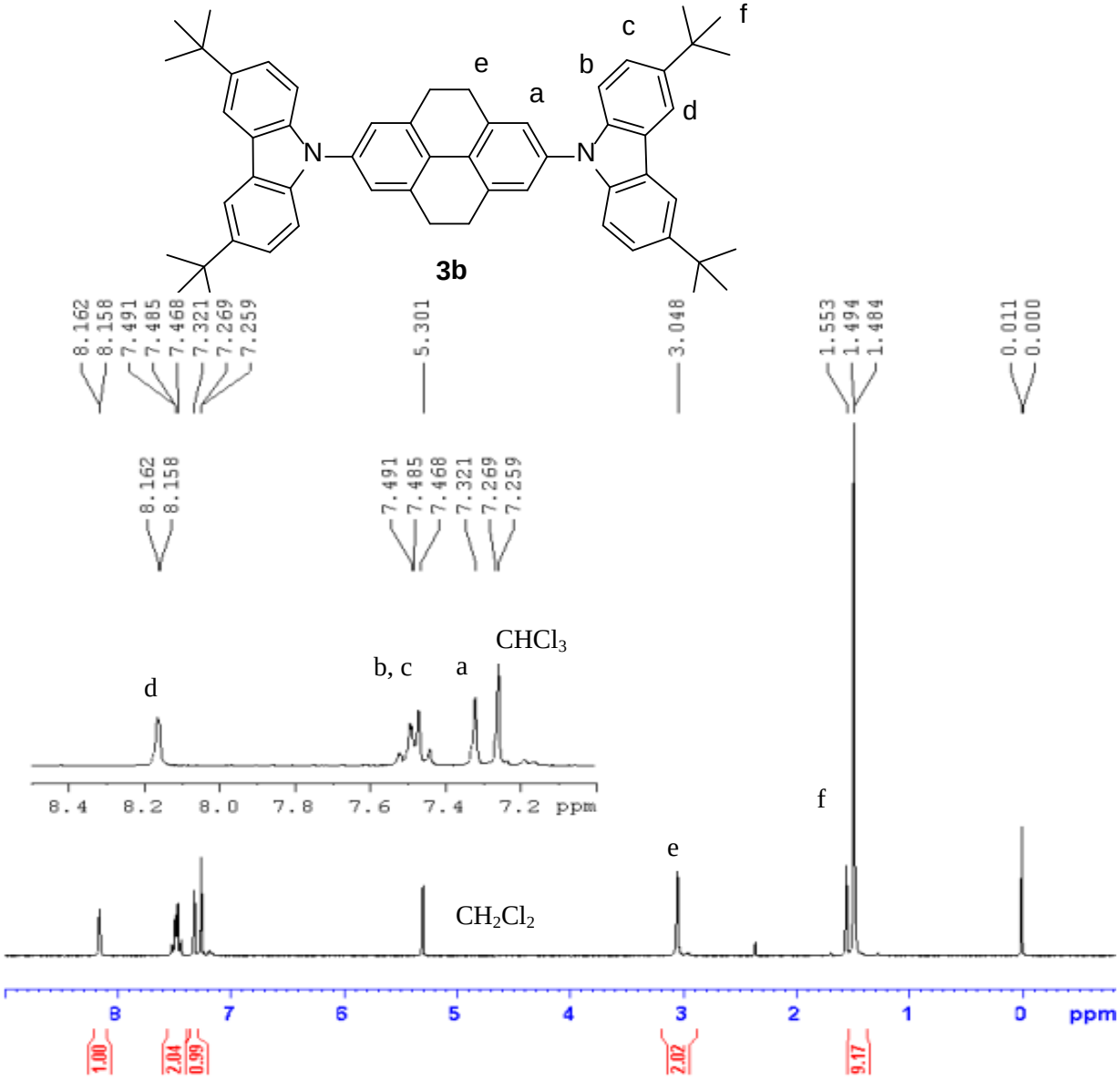

Figure S18.^{1}H NMR of 2,7-bis(3,6-di-*tert*-butylcarbazol-9-yl)tetrahydropyrene (**3b**) in $CDCl_3$.

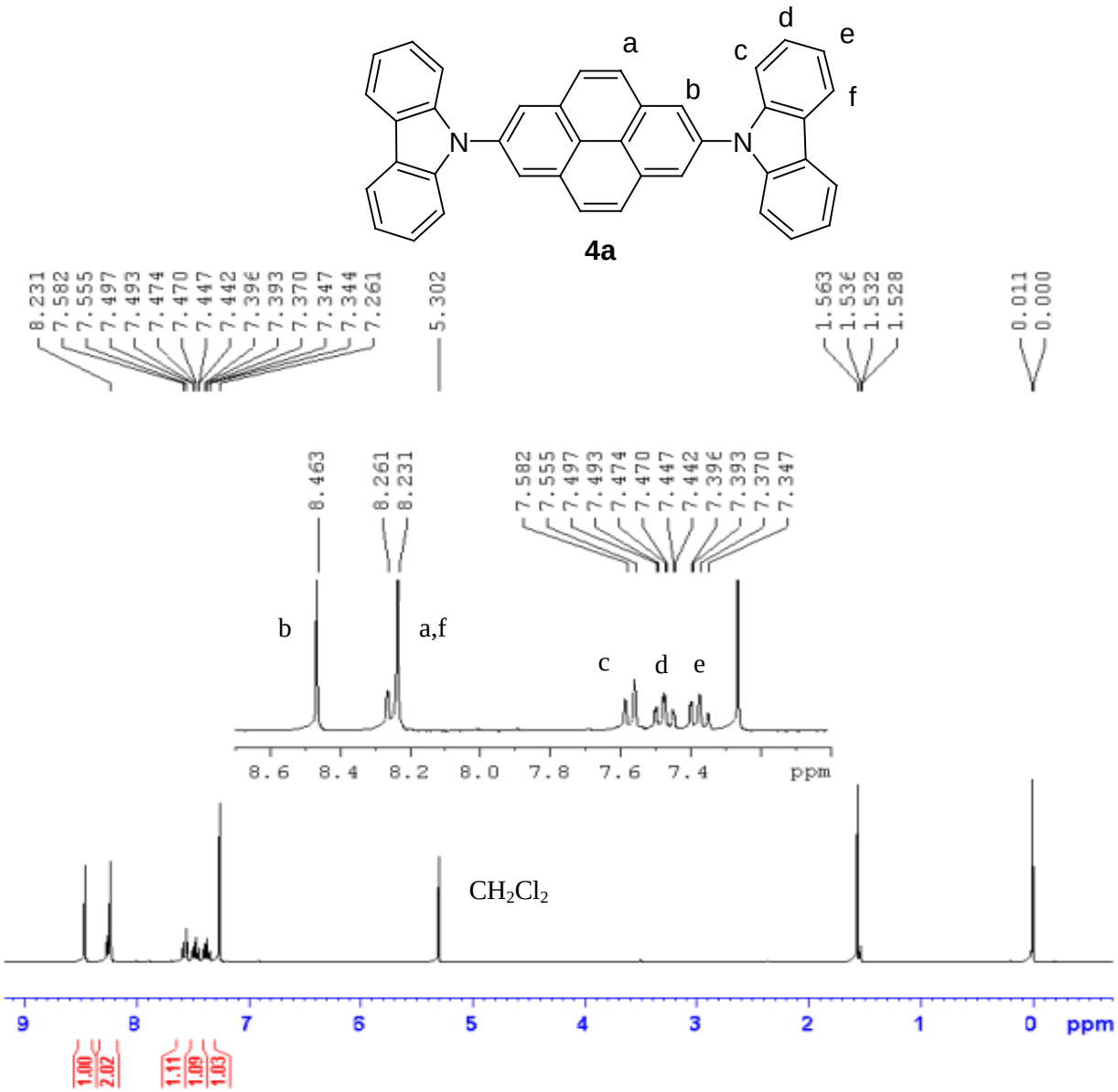

Figure S19.^{1}H NMR of 2,7-bis(carbazol-9-yl)pyrene (**4a**) in $CDCl_3$.

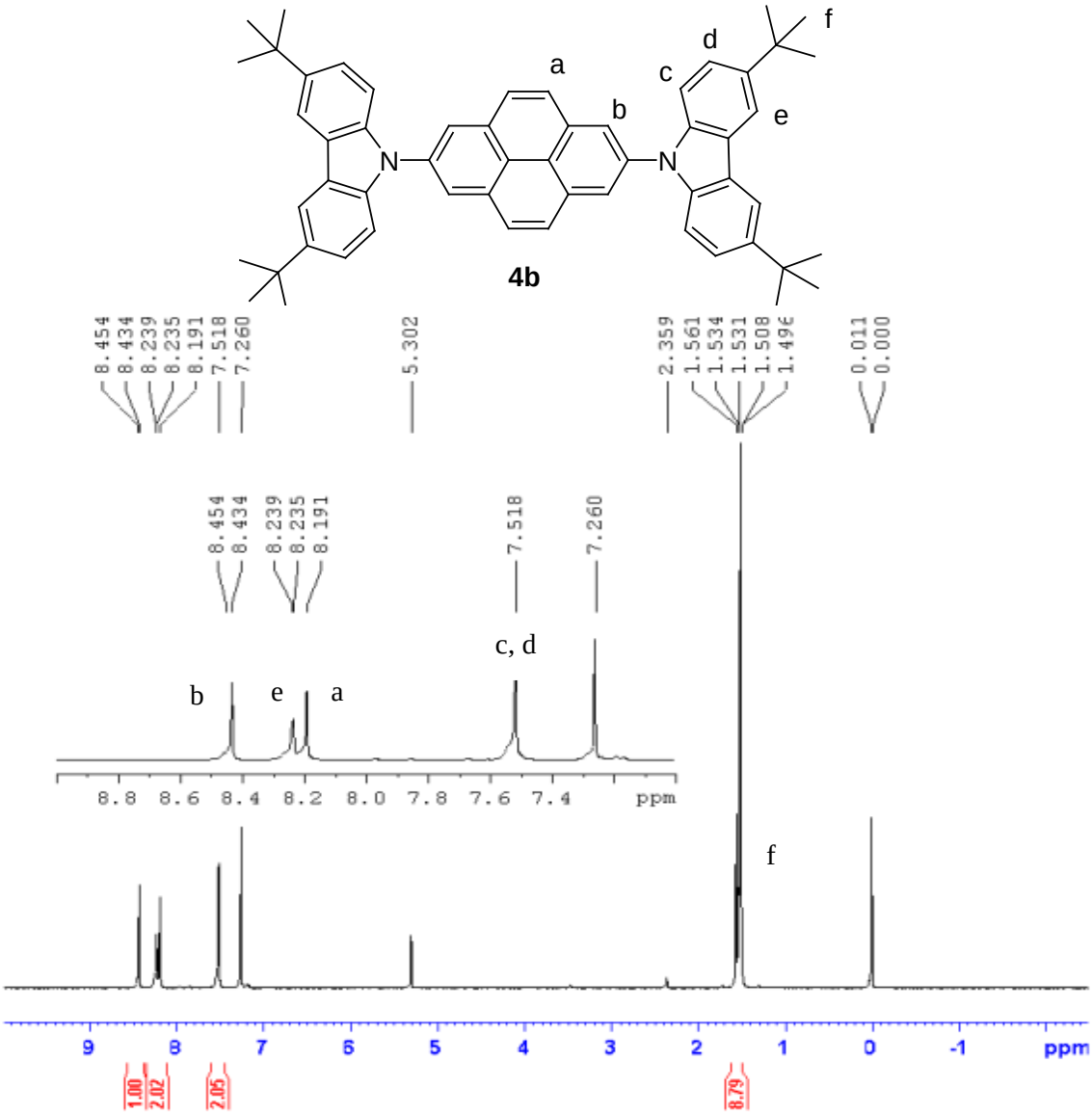

Figure S20. ^{1}H NMR of 2,7-bis(3,6-di-*tert*-butylcarbazol-9-yl)pyrene (**4b**) in $CDCl_3$.

References

1. The largest R. M. S. deviation of fitted atoms for carbazole group is observed for **4a**: 0.05 Å; for bridging six-membered ring is observed for **2a**: 0.04 Å.
2. P. J. Low, M. A. J. Paterson, D. S. Yufit, J. A. K. Howard, J. C. Cherryman, D. R. Tackley, R. Brook and B. Brown, *J. Mater. Chem.*, 2005, **15**, 2304-2315.
3. W. Li, J. Qiao, L. Duan, L. Wang and Y. Qiu, *Tetrahedron*, 2007, **63**, 10161-10168.
4. M. A. Reddy, A. Thomas, B. Sridha, V. J. Rao and K. Bhanuprakash, *Tetrahedron Lett.*, 2011, **52**, 6942-6947.
5. W. Wu and J. Tong, *Acta Crystallogr.*, 2011, **E67**, o1919.
6. S. Saha and S. Samanta, *Acta Crystallogr.*, 1999, **C55**, 1299-1300.
7. The crystal structures of **1a**, **2b**, **4a**, and **4b** have been deposited at the Cambridge Crystallographic Data Centre and allocated the deposition numbers CCDC 899423, 899424, 899425, and 899426, respectively.
8. A. Sharma and S. Schulman, *Introduction to Fluorescence Spectroscopy*, Wiley-Interscience, USA, 1999.
9. C. A. Parker, P*hotoluminescence of Solutions with Applications to Photochemistry and Analytical Chemistry*, 1968.
10. U. Subuddhi, S. Haldar, S. Sankararaman and A. K. Mishra, P*hotochem. Photobiol. Sci.*, 2006, **5,** 459-466.
11. J. R. Lakowicz, P*rinciples of Fluorescence Spectroscopy*, Kluwer Academic, Plenum Publishers, NewYork, 1999.